ELSEVIER

Advances in Water Resources 24 (2001) 213–224

Advances in Water Resources

www.elsevier.com/locate/advwatres

# Rainfall forecasting using variational assimilation of radar data in numerical cloud models

Mircea Grecu, Witold F. Krajewski *

*Iowa Institute of Hydraulic Research, The University of Iowa, Iowa City, IA 52242, USA*

Received 27 December 1999; received in revised form 30 July 2000; accepted 2 August 2000

**Abstract**

In this paper, a variational data assimilation procedure for initialization of a cloud model using radar reflectivity and radial velocity observations and its impact on short term rainfall forecasting are investigated in a simulation framework. The procedure is based on the formulation of an objective function, which consists of a linear combination of the squared differences between model forecasts and actual observations. The model's initialization requires the gradient-based minimization of the objective function. Three sources of errors in assimilation and forecasting are considered. These include observational errors, mathematically ill-posed structure (the observations are incomplete and do not uniquely determine the cloud model's initial conditions) and optimization related issues (the observations are complete, but the optimization procedure involved in the initialization fails to find the best solution). It is found that the reflectivity observation errors have significant impact on forecasts and that the mathematical structure and optimization caused errors are related. Conclusions and recommendations for future work are formulated. 

*Keywords:* Variational methods; Data assimilation; Cloud models; Rainfall forecasting

## 1. Introduction

In this paper we investigate the use of variational assimilation (VA) of radar data for rainfall forecasting based on cloud models. VA is an effective technique that uses physically based models to determine variables that are not currently measured. For example, Sun and Crook [17] formulated a VA framework based on a cloud model, Doppler velocity and radar reflectivity observations, that allows the retrieval of velocity, temperature, pressure, and various species of water in the radar measurement domain. Bao and Warner [2], Verlinde and Cotton [20], and Sun and Crook [16] all include other examples of atmospheric variable retrievals based on indirect observations. With the advent of high-resolution weather radar systems such as WSR-88D [12], which provide a spatial resolution of about 1 km every 4–6 min, VA of radar data has become a useful tool in numerical rainfall forecasting. Radar observations may be used to initialize cloud models, which can then be used for forecasting.

Many of the questions related to the VA of radar data in cloud models cannot be answered by theoretical considerations and require numerical investigations. This is because, even if the cloud model is assumed perfect and the radar observations are error-free, the estimation (retrieval) of the initial conditions is subject to errors. These errors have a mathematical character (when the initial conditions cannot be determined uniquely based on the actual observations) or a numerical character (when the numerical procedures fail to determine accurately an existing unique set of initial conditions). There is no theoretical basis that provides the error quantification, and this justifies the use of numerical experiments. Sun and Crook [17] characterized the VA retrieval errors, but they did not investigate the effect of these errors on forecasting. In this paper, we address this issue, namely, the effect of VA retrieval errors on rainfall forecasting at storm scales. Also, we discuss the mathematical and numerical character of the errors and suggest a strategy to minimize them.

To achieve the objectives of the paper, we simulated a rainfall event using a 2-D cloud model. Then, using the cloud model output, we produced several sets of radar reflectivity and Doppler velocity observations. Based on these observations, various assimilation

* Corresponding author. Fax: +1-319-335-5238.
*E-mail address:* witold-krajewski@uiowa.edu (W.F. Krajewski).

0309-1708/00/$ - see front matter 
PII: S0309-1708(00)00046-4

experiments were performed according to different formulations of the objective function in the VA framework. We initialized the cloud model using the retrieval provided by the VA technique and ran it forward to make forecasts. Based on the comparisons between the output of the VA initialized runs and the reference output, we characterized and studied the accuracy of the forecasting.

The paper is organized as follows. In Section 2, we describe the cloud model used in the paper. Section 3 contains the VA formulation. In Section 4, we present the particular scenarios investigated and analyze the results. In Section 5, in the summary, we formulate conclusions.

## 2. Numerical simulation of a storm

The cloud model used in the paper is based on the Navier–Stokes equations augmented with equations for the conservation of internal energy, and conservation of mass of three species of water (water vapor, cloud and rain water). Using the anelastic approximation [10], the momentum equations become

$$\frac{\mathrm{D}\tilde{\rho}u_i}{\mathrm{D}t} = -\frac{\partial p^*}{\partial x_i} + \tilde{\rho}B\delta_{i3} + \nu\nabla^2\tilde{\rho}u_i, \tag{1}$$

where $u_i$ is the $i$th component of velocity, $\tilde{\rho}$ the mean density of air (function only of altitude), $p^*$ the pressure deviation, $B$ the buoyancy, and $\nu$ is the dynamic viscosity. Superscript "*" indicates the deviation from a reference state symbolized by "$\circ$". The buoyancy is defined as [10]

$$B = g\left(\frac{T^*}{T^\circ} - \frac{p^*}{p^\circ} - 0.61q_\mathrm{v}^* - q_\mathrm{c} - q_\mathrm{r}\right), \tag{2}$$

where $q_\mathrm{v}$, $q_\mathrm{c}$, $q_\mathrm{r}$ are the mixing ratios of water vapor, cloud water, and rain water, and $T$ is the temperature. The continuity equation is

$$\frac{\partial\tilde{\rho}u_i}{\partial x_i} = 0 \tag{3}$$

and the conservation of internal energy may be written as

$$\frac{\mathrm{D}\tilde{\rho}T}{\mathrm{D}t} = -u_3\frac{\tilde{\rho}g}{C_\mathrm{p}} + k\nabla^2\tilde{\rho}T^* + S_\mathrm{T}, \tag{4}$$

where $k$ is the diffusivity of temperature, $C_\mathrm{p}$ the heat capacity of water vapor at constant pressure, and $S_\mathrm{T}$ is a thermal source/sink due to condensation/evaporation of water. We will describe later how $S_\mathrm{T}$ is determined. The reasons for considering $T^*$ instead of $T$ in the diffusion terms are explained in [22]. The equations that describe the conservation of water are

$$\frac{\mathrm{D}q_\mathrm{v}}{\mathrm{D}t} = -S + E + D_{q_\mathrm{v}}, \tag{5}$$

$$\frac{\mathrm{D}q_\mathrm{c}}{\mathrm{D}t} = S - A - C + D_{q_\mathrm{c}}, \tag{6}$$

$$\frac{\mathrm{D}q_\mathrm{r}}{\mathrm{D}t} = \frac{1}{\tilde{\rho}}\frac{\partial}{\partial z}\left(\tilde{\rho}V_\mathrm{r}q_\mathrm{r}\right) + A + C - E + D_{q_\mathrm{r}}, \tag{7}$$

where $S$ is the source of cloud water due to condensation, $A$ the autoconversion, $C$ the collection of cloud water, $E$ the precipitation evaporation, and $D_q$ represents diffusion terms. We denote raindrop terminal velocity $V_\mathrm{r}$. It may be determined as $V_\mathrm{r} = 21.9(\tilde{\rho}q_\mathrm{r})^{0.125}$, with $V_\mathrm{r}$ in m/s, $\tilde{\rho}$ in g/cm$^3$, and $q_\mathrm{r}$ in g/g [15]. We model the terms $A$, $C$, and $E$ according to Kessler's [11] parameterization: $A = \max(0, \alpha_\mathrm{c}(q_\mathrm{c} - q_\mathrm{crit}))$, where $\alpha_\mathrm{c} = 0.001\ \mathrm{s}^{-1}$ and $q_\mathrm{crit} = 1.5$ g/kg; $C = \gamma q_\mathrm{c}q_\mathrm{r}^{0.95}$, where $\gamma = 0.002\ \mathrm{s}^{-1}$; and $E = \max(0, -\beta(q_\mathrm{v} - q_\mathrm{vs}))$, where $\beta = 0.001$ and $q_\mathrm{vs}$ is the water vapor mixing ratio at the cloud temperature and pressure. We determined condensation $S$ through a moist adjustment process [17] such that the physical condition $q_\mathrm{v} \leqslant q_\mathrm{vs}$ is always satisfied, where $q_\mathrm{vs}$ is the saturation water vapor mixing ratio, which may be determined using Teten's formula [21]

$$q_\mathrm{vs} = 0.662 \cdot 6.11\frac{\exp\left(17.26\frac{T-273.16}{T-35.86}\right)}{p}, \tag{8}$$

where $p$ is the pressure in mbar. Based on the $S$ and $E$, $S_\mathrm{T}$ may be determined as

$$S_\mathrm{T} = \frac{L}{C_\mathrm{P}}(S - E), \tag{9}$$

where $L$ is the latent heat of vaporization, which is considered constant.

We implemented numerical models (1)–(9) for a two-dimensional $x$–$z$ domain with size of $34\times17$ km$^2$. The domain was discretized using a $34\times34$ orthogonal uniform grid ($\Delta x = 1$ km and $\Delta z = 0.5$ km). Velocity, temperature, air density, and water contents were defined at the points, while the centers of the grid cells were used for pressure. This grid layout is the same as in the study of Lee and Leone [13], but a finite difference scheme is used instead of the original finite element formulation. We adopted this staggered scheme to provide a consistent discretization that satisfies the continuity equation up to the machine precision [6].

To discretize the transport equations (Eq. (1)), we use a two-step Lax–Wendroff scheme [18]. That is, we treat sequentially each component of the advection terms in transport equations, using a Lax–Wendroff scheme corresponding to a 1-D problem. The advantages of using this numerical scheme are in its simplicity and second-order precision both in time and space.

We use a multi-step algorithm to integrate the cloud model. First, consider the momentum equation (1). Note that the pressure is not known in (1) because there is no dynamic equation for it. We use a formulation similar to that of Chorin [4] to determine the pressure

based on the continuity equation. That is, we introduce approximate values of pressure in (1) to calculate the new velocity values. These values do not satisfy the continuity equation. Then, we derive and solve a pressure correction equation that, when applied to the velocity field, makes it satisfy the continuity equation. After the momentum equations, we consider the transport equations of the three phases of water, assuming that the conversion terms $A$, $C$, $E$, and $S$ are zero. In the next step, we check every grid point to see whether saturation occurred. If it did, we perform a moisture adjustment [17]. We adjust the moisture by reducing the water vapor cloud content to the saturation level, and increasing the cloud content by the same amount. At the same time, the temperature is modified according to the heat conservation principle. Finally, we update the water mixing ratios using the Kessler's parameterization. This parameterization accounts for rain evaporation in subsaturated regions. Consequently, the temperature decreases in those regions due to heat absorbed during the process. These changes in temperature are also taken into account by the numerical model. That is done by simultaneously solving the modified forms of Eqs. (4)–(8) that ignore transport and diffusion. In this respect, a Newton–Raphson procedure [1], which requires the gradients of the terms in the equations, is used.

We initialized the model using the sounding data shown in Fig. 1, which is a description of an event in Del City, Oklahoma, on 20 May 1977. In this paper, we did not consider the wind shear in the sounding. This was justified by the fact that an initially sheared wind field leads to more complex developments, such as multiple rain cells, stretching of rain cells etc., that would require an increase of the computational domain. On the other hand, a VA approach requires several times more memory and computational time than the dynamic model on which it is based. Consequently, we considered the initial wind field to be zero.

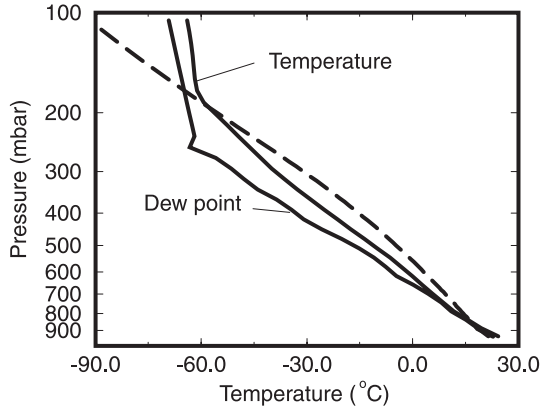


Fig. 1. Sounding data. The dashed line represents the temperature of an air parcel raised from the surface. The other two lines are for the temperature and dew point.

We initialized the model using a thermal perturbation, 8 km wide and 4 km deep, in the middle of the computational domain. The perturbation consisted of 3 K temperature excess. The boundary conditions were zero for the velocities normal to boundaries. All the other variables had the derivatives zero normal to the boundaries. The eddy viscosity in Eq. (1) was set to 150 $m^2\ s^{-1}$, and $k$ to $3\nu$. The diffusivity of water in Eqs. (5)–(7) was assumed to be equal to $3\nu$. These values are typical for numerical cloud models [17]. The time-step was 10 s.

Based on the simulation described above, we conducted variational retrieval experiments. We synthesized, using the numerical cloud output, sets of radar reflectivity and Doppler velocity observations. We used the relationship [17]

$$Z = 2.4 \cdot 10^6 (\tilde{\rho} q_r)^{1.75} \tag{10}$$

to determine the reflectivity factor $Z$ from rain water mixing ratio. Relationship (10), which is valid for a Marshall Palmer distribution of rain drop sizes, may be derived by expressing the rain dropsize distribution's exponent $\Lambda$ as a function of $Z$ and using it in the definition of $q_r$. We calculated the Doppler velocity at a location $(x,z)$ using [17]

$$V_D = u\frac{x - x_r}{r} + (w - V_r)\frac{z - z_r}{r}, \tag{11}$$

where $r$ is the distance from $(x,z)$ to the radar, whose coordinates are $(x_r, z_r)$. We arbitrarily set $x_r = -40$ km and $z_r = 0$ km. Based on the simulated radar data, we used the VA technique to initialize the cloud model in agreement with the observations. Then, the cloud model was run forward to make forecasts, and we compared its output to the reference run. Based on the comparisons, we were able to make performance assessments.

## 3. Variational assimilation technique

### 3.1. General formulation

Although detailed presentations of VA formulations may be found in several papers (see for example [19] or [3]), this section includes a brief account of our VA formulation to facilitate the identification of the error-related issues. We rewrite the cloud model presented above in a generic, discrete form as

$$X^{i+1} = F(X^i), \tag{12}$$

where $X^i$ is the state vector variable (containing the complete information to fully describe the model's physical state in space and time), and $F$ is the model that describes the system evolution. Suppose that a set of $M$ measurements at different times $t_{i_k} = i_k \Delta t$, where $\Delta t$ is the time step and $i_k$ are positive integers, is available

$$Y^{i_k} = H(X^{i_k}) + \varepsilon_{i_k} \quad k \in \{1, 2, \ldots, M\}, \tag{13}$$

where $Y^{i_k}$ are the measured variables and $\varepsilon_{i_k}$ are Gaussian errors with known characteristics. We use the two-level index notations to indicate that the observations do not have to be regular in time. We want to initialize the cloud model at time $t_{i_1}$, such that the model output obtained by applying Eq. (12) repeatedly is in agreement with observations (13). Thus, an objective function may be defined as follows:

$$J = \sum_{k=1}^{M} (Y^{i_k} - H(X^{i_k}))^{\mathrm{T}} W_{i_k}^{-1} (Y^{i_k} - H(X^{i_k})), \tag{14}$$

where $W_{i_k}$ is a square weight matrix. This problem can be reduced to a search for the variable $X_{i_1}$ that minimizes (14) with constraints (12). Objective function (14) may be expressed exclusively as a function of $X_{i_1}$, and its gradient with respect to $X_{i_1}$ becomes

$$\nabla J = -2 \sum_{k=1}^{M} (Y^{i_k} - H(X^{i_k}))^{\mathrm{T}} W_{i_k}^{-1} \nabla H^{i_k} \nabla F^{i_k - 1} \cdots \nabla F^{1}, \tag{15}$$

where, for simplicity of notation $\nabla F(X^i) = \nabla F^i$ and $\nabla H(X^i) = \nabla H^i$. Then, a gradient-based optimization technique may be used to determine the initial condition $X_{i_1}$ that minimizes (14). The efficient evaluation of the expression on the right-hand side of (15) requires the development of a special model, called the *adjoint*, from the forward model (12). The adjoint model allows for the calculation of the product on the right-hand side of (15) starting from the right-most term, which is a vector. In this way, matrix-by-matrix multiplications are replaced by matrix-by-vector multiplications, which are one order of magnitude less computer-intensive. However, the development of the adjoint model is difficult. In this paper, we used the automatic code of Gering and Kaminski [8] to derive the adjoint model from the forward one. Once evaluated, gradient (15) may be used by an optimization procedure to determine the initial condition $X_{i_1}$. Consequently, we used a special optimization procedure, namely the limited memory Broyden–Fletcher–Goldfarb–Shanno (BFGS) procedure of Liu and Nocedal [14], which is efficient for a large number of variables.

By analyzing the above methodology for initializing a model in presence of observations, we identified several potential difficulties associated with the problem. First, the observations may not contain sufficient information to uniquely determine the minimum of (14), i.e. $X_{i_1}$. In this situation, the optimization algorithm would find an arbitrary solution that might be far from the optimal one. Second, although a unique solution of (14) exists, that is, the model initial conditions may be retrieved exactly, the optimization procedure might not able to locate it precisely, due to the large number of variables, which for the current problem is 6936. Even the most effective optimization algorithm may fail for this number of variables and extremely complex and nonlinear functions such as (14). We considered the limited memory BFGS optimization algorithm used in this paper as the best option one has for this type of problem, and, consequently, acknowledged this second pitfall as an objective fact, but not simply a consequence of the particular optimization technique used in the paper.

### 3.2. Objective function definition

For the current problem, the measurements may be decomposed into two disjoint sets of observations, namely, reflectivities and Doppler velocities, and, consequently, the objective function may be rewritten as a function of two terms. That is

$$J = \sum_{k=1}^{M} \left(Z^{i_k} - Z^{i_k,\mathrm{obs}}\right)^{\mathrm{T}} W_{Z,i_k}^{-1} \left(Z^{i_k} - Z^{i_k,\mathrm{obs}}\right) + \sum_{k=1}^{M} \left(V_{\mathrm{D}}^{i_k} - V_{\mathrm{D}}^{i_k,\mathrm{obs}}\right)^{\mathrm{T}} W_{V,i_k}^{-1} \left(V_{\mathrm{D}}^{i_k} - V_{\mathrm{D}}^{i_k,\mathrm{obs}}\right). \tag{16}$$

We used superscript "obs" to indicate the observed values ($Y$ in (14)), and obtained the other values via operator $H$, defined in Eqs. (10) and (11). We evaluated the errors of (16) at each grid point. In practice, given the limited vertical resolution of radars, this approach might not be accurate, and functional forms for $H$, more complex than those in (10) and (11), need to be considered. Choosing the weight matrices $W_{Z,i_k}$ and $W_{V,i_k}$ is a difficult task. We describe the methodology we used to determine them in the next section.

Sun and Crook [17] considered two additional terms in (16): a background and a penalty. They found that these terms improve the retrieval accuracy. In the preliminary stages of our study, we did not find a significant improvement in forecasting due to background and penalty terms, and consequently, we did not consider these terms further. The background term becomes important when $M$ is a large number (which is not the case either in our study or in [17]). This situation corresponds to a long sequence of observations, which occur in real situations. Then it is impractical to consider all available observations. Also, the effect of model inaccuracy may increase considerably, because the errors in models propagate in time. It is therefore rational to consider only a small number of observations (three or four) and to account for the information provided by prior observations through a background term. This strategy might be rigorously formulated in a optimal way [7]. However, for the number of variables considered in the current problem (6936), the necessity of calculating and storing the weight matrix for the background term poses many problems. The weight matrix in this case is a measure of the uncertainty concerning the accuracy of

estimates provided by prior measurements. Therefore, we considered only three or four sets of observations, and did not investigate the background term issue. Nevertheless, this aspect needs to be addressed in future studies.

## 4. Results

As specified in Section 3, we numerically simulated a storm using a 2-D implementation of the cloud model presented above. Based on the cloud variables, we synthesized radar observations at different times. We considered the cloud model's variables, i.e. velocity, pressure, temperature, cloud, vapor and rain mixing ratio, to be unknown, and applied the variational assimilation technique to estimate them based on the observations. We compared the estimated values to the true (reference) ones, and, based on the comparisons, we evaluated the approach performance.

We set the initial conditions in the assimilation procedure as follows. The velocity field and the temperature deviation were zero. The sounding values were assigned to the water vapor field wherever there was no rain. In the areas with rain, we specified the saturation water vapor content corresponding to a certain excess of temperature (0 or 2 K) relative to the sounding temperature. We considered the cloud content to be zero everywhere, and estimated the rain water directly from the radar measurements. This is not the only way to initialize the assimilation procedure. Although the number of iterations that the optimization procedure needs to perform to achieve convergence depends greatly on the initial conditions, the only requirement that must be satisfied concerns the objective function derivatives. They must be nonzero. It is possible that the initial conditions are such small deviations from the sounding values that no sensitivity is noticed in the objective function. One example in this direction is a thermal perturbation in a dry environment which is not big enough to trigger phase conversion and sustain the convection. In this situation, the derivative of the objective function with respect to the initial conditions would be zero, because the environment remains dry while the observables are based on precipitation. This justifies selecting the initial conditions in order to cause phase conversion to take place in the assimilation interval with precipitation as nonzero at its end. The initial conditions proposed here meet this requirement.

Determining matrices $W$ in the objective function is not a trivial task, even if the statistical properties of the observational errors are known precisely. This is because inversion problems, i.e. determining a set of variables based on incomplete observations, are generally ill posed. They do not have a unique solution, or the solution is not stable to small perturbations. Even if the observations are error-free, it is impossible to rigorously formulate an objective function that would provide the best estimate of the problem variables. In these conditions, the only alternative is the use of heuristic approaches. In this paper, we considered the observational errors to be uncorrelated. This is consistent with the way the observations were generated in the current numerical experiments, but does not necessarily correspond to real situations. However, in real applications, the error in radar observations can be estimated [5] and a methodology similar to the one presented here may be used. Since the errors were considered to be uncorrelated, we chose matrices $W_{Z,i_k}^{-1}$ and $W_{V,i_k}^{-1}$ proportional to the identity matrix. In real situations the identity matrix may be replaced with appropriate matrices provided by the analysis of the error structure. Then we determined two proportionality constants (because the objective function is a linear combination of the two constants), with just one being independent. We started with proportionality constants that provided the equality of the two terms of the objective function. We modified one proportionality constant, performed the assimilation, and evaluated the results until we discovered the best performance. We noticed quite a large interval for which the magnitude of the proportionality constant changed several times without significant changes in performance. In conclusion, the objective function is defined as a linear combination of the squared errors evaluated at every point of the computational grid, where the weights were defined based on a heuristic methodology.

We investigated the performance of the variational assimilation framework presented above in a series of cases. These cases were devised to reveal the influence of observational errors, and the length of the assimilation interval, on performance. We also tried to identify the cause of errors in estimating the cloud initial conditions. The cases are listed in Table 1. The four sets of measurements are 4.16 min apart (comparable with the temporal resolution of real radar systems, but also a multiple of the time-step, which is 10 s). The assimilation interval is $[12.50, 25.00]$ min in the cases with four measurement sets, and $[16.67, 25.00]$ min in the cases with three measurements sets. The error model used for velocity observations was, in case C2,

$$V_e^{obs} = V^{obs}(1 + v_V), \tag{17}$$

where $V_e^{obs}$ is the observed radial velocity, $V^{obs}$ the synthesized radial velocity, and $v_V$ is random noise, normally distributed with 0 mean and 0.2 standard deviation. The radar reflectivity observations were corrupted with noise in case C3 as

$$Z_e^{obs} = Z^{obs} + v_Z, \tag{18}$$

where $Z_e^{obs}$ is the observed reflectivity, $Z^{obs}$ the synthesized reflectivity and $v_Z$ is random noise, normally distributed with 0 mean and 3 dBZ standard deviation. We included

case C4 in the analysis to study the influence of the optimization initial solution on the performance. In other words, we analyzed the sensitivity of the optimization solution on the initial guess. We considered case C5 to characterize the effect of the length of the assimilation interval on the forecasting performance. The estimation of the cloud initial conditions, should, at least in theory, be better in C1 than in C5, because more information is

Table 1
Description of the cases investigated in the assimilation experiments

| Case | Description |
|---|---|
| C1 | Four sets of observations 4.16 min apart, no observational errors, the initial temperature deviation of the cloud set to a 2 K excess |
| C2 | Same as for C1, but with errors in velocity observations |
| C3 | Same as for C1, but with errors in reflectivity observations |
| C4 | Same as for C1, but with the initial temperature deviation of the cloud set to a 0 K excess |
| C5 | Three sets of observations, no observational errors, the initial temperature deviation of the cloud set to a 2 K excess |
| C6 | Same as for C1, but without optimization |
| E1 | Same assimilation interval as for C1, but with 100 sets of observations 10 s apart |
| E2 | Same as for E1, but with temperature observations included in the objective function |

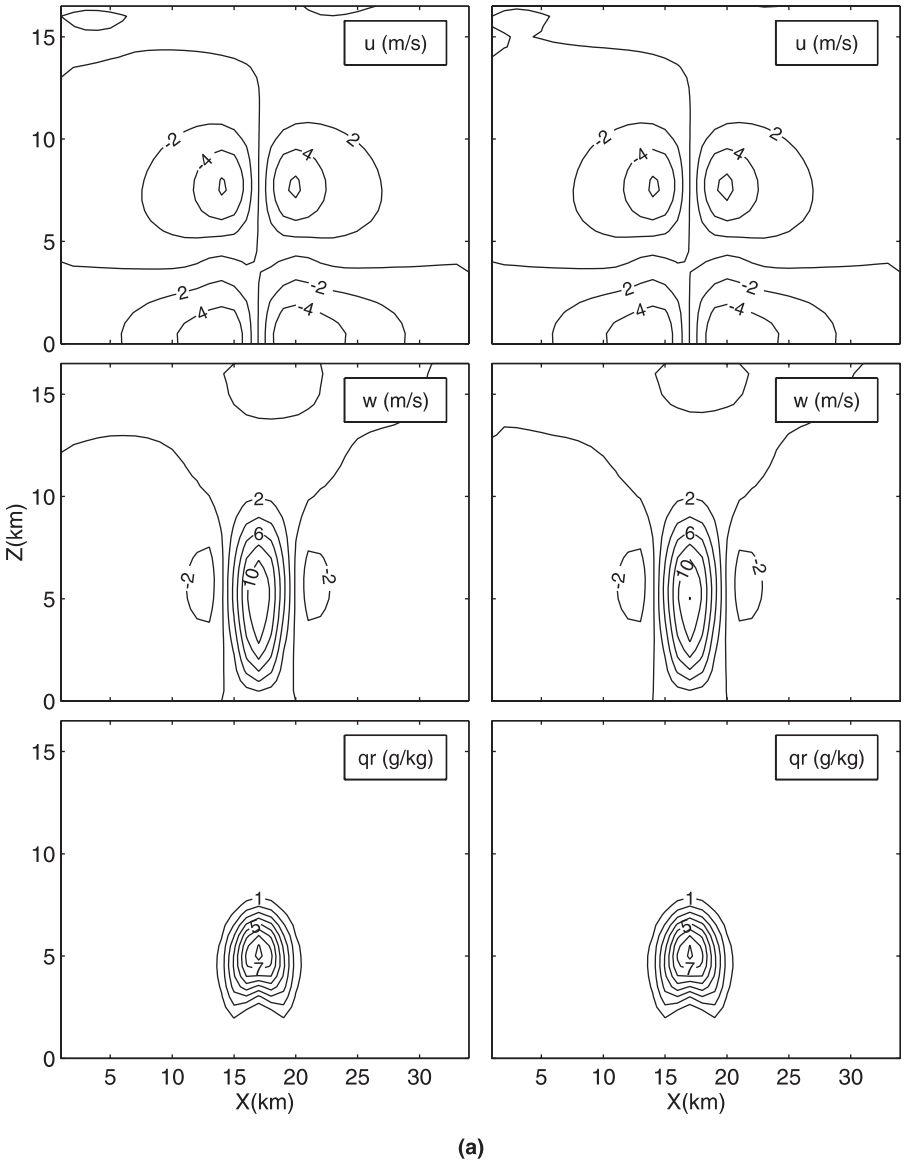


Fig. 2. Reference and retrieved cloud variables at time $t = 25.00$ min. Left column represents the reference variables and the right column represents the retrieved variables: (a) horizontal velocity, vertical velocity, and rain water mixing ratio; (b) temperature deviation, deviation of water vapor mixing ratio, and cloud water mixing ratio.

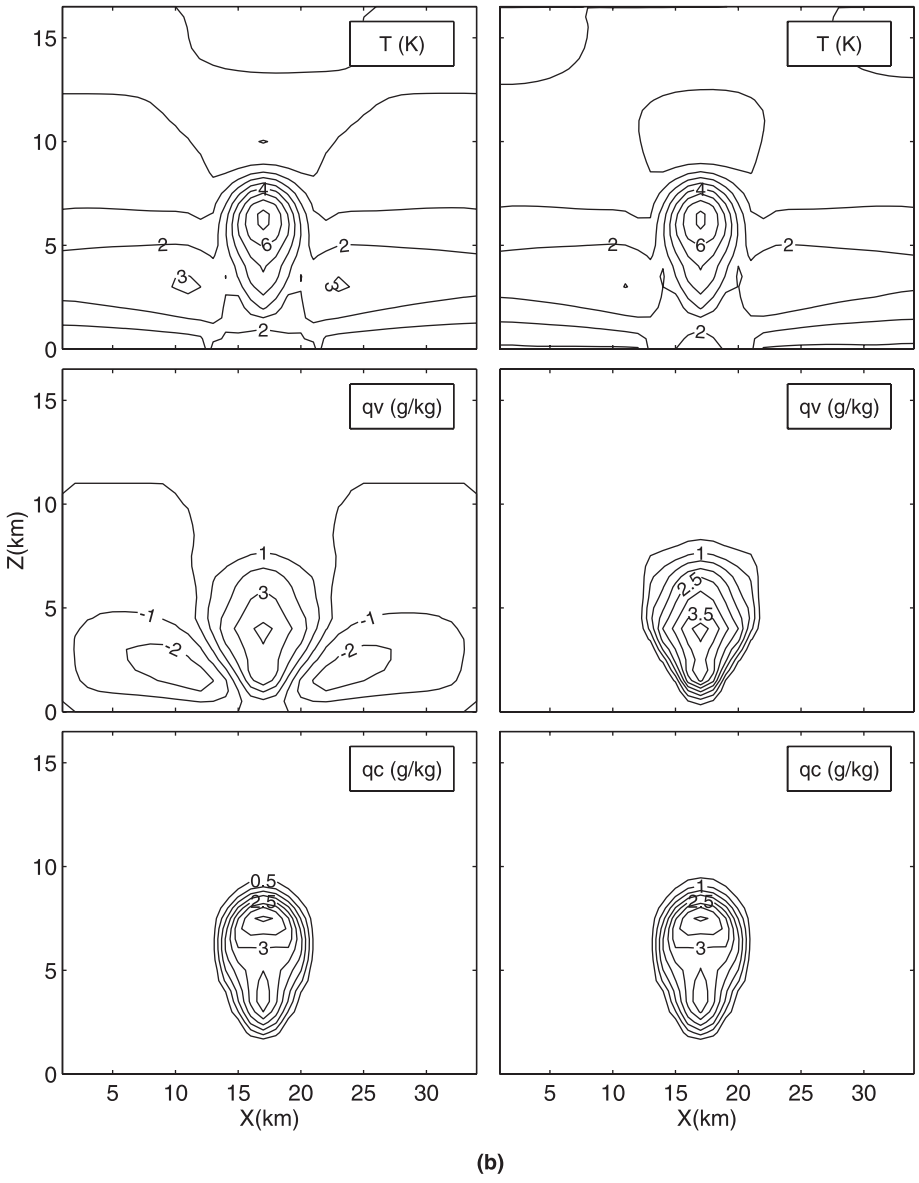


Fig. 2 (*continued*)

available. Case C6 was used to indirectly characterize the effectiveness of the optimization procedure. By comparing the results of C6 and C1 we could infer whether the use of the optimization procedure was justified. Cases E1 and E2, although not realistic from the practical standpoint, were devised to identify the contributions of ill-posedness (incomplete information) and optimization limitations in the errors. Case E1 is not different from C1 in terms of the assimilation interval and accuracy of observations, but in terms of observations' frequency. That is, the radar measurements were considered available every 10 s, which is the time step of the numerical model. Therefore, 25 times more observations than in C1 were used in case E1. Case E2 is similar to E1, but temperature observations were included in the objective function. The objective function became

$$J_{\mathrm{T}} = J + \sum_{k=1}^{M} \left(T^{i_k} - T^{i_k,\mathrm{obs}}\right)^{\mathrm{T}} W_{T,i_k}^{-1} \left(T^{i_k} - T^{i_k,\mathrm{obs}}\right),$$

where $J$ was defined in (16). The weight matrices $W_{T,i_k}$ were determined from $W_{z,i_k}$ by multiplication with factor $Z_{\mathrm{m}}/T_{\mathrm{m}}$, where $Z_{\mathrm{m}}$ is the mean of the observed reflectivities and $T_{\mathrm{m}}$ is the mean of the observed temperatures. This strategy is acceptable when the observations are error-free and makes the optimization problem better conditioned [1], because the terms involved in the objective function are on the same order of magnitude.

Illustrations of the retrieved cloud variables for C1 at $t = 25$ min are given in Fig. 2. The reference values are represented in the left column and the retrieved ones in the right column. It may be observed that the assimilation procedure is able to reproduce the storm

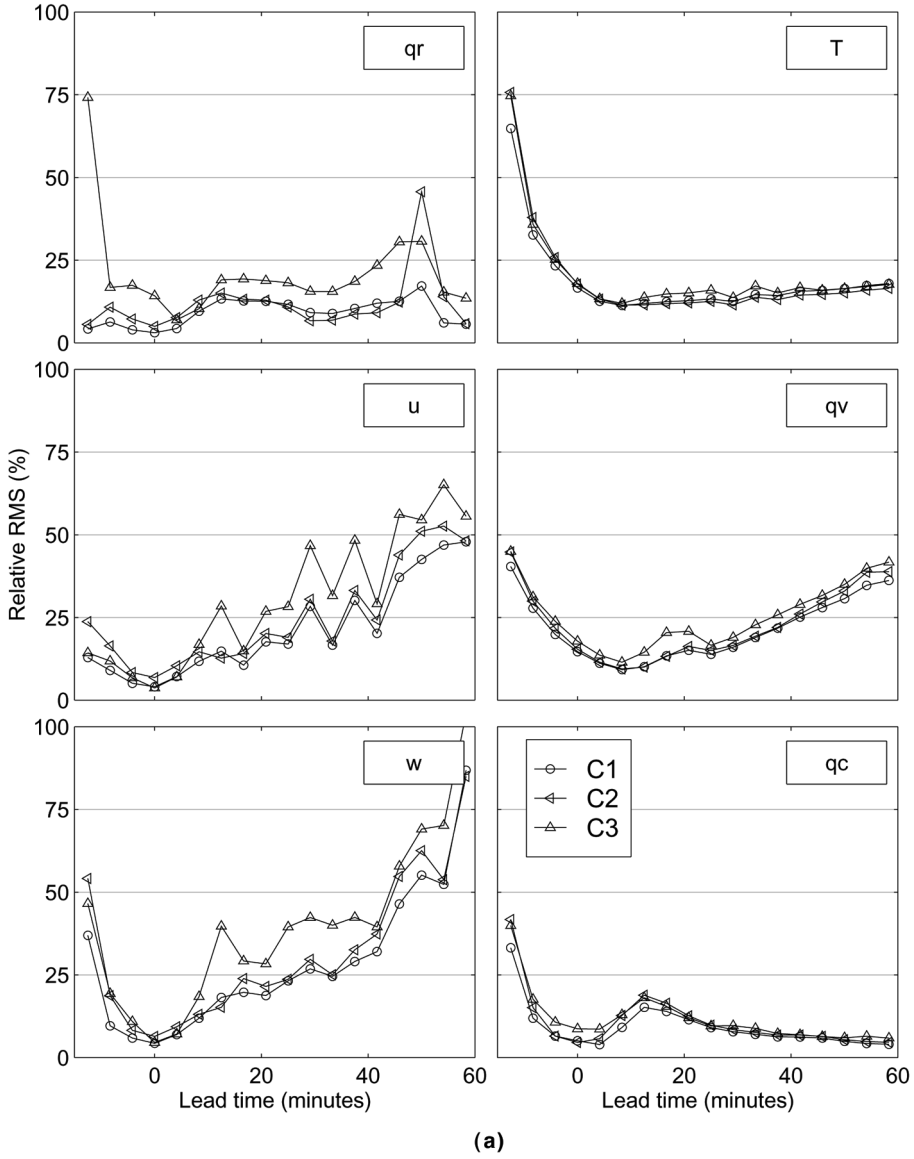


Fig. 3. Relative root mean squared error of retrieved/forecasted variables as a function of time. From top to bottom, left to right: rain water mixing ratio, horizontal velocity, vertical velocity, temperature deviation, deviation of water vapor mixing ratio, and cloud water mixing ratio: (a) cases C1, C2, and C3; (b) cases C1, C4, C5, and C6.

characteristics quite well. This is quite impressive, considering that, for example, the initial flow field is zero. The retrieved temperature, cloud water, and rain patterns also agree with the reference. Time $t = 25$ min corresponds to the end of the assimilation interval. Obviously, there are differences between the estimated and the reference values. The most pronounced ones are those corresponding to the deviation of the water vapor content from the environmental values.

We have shown quantitative results describing the performance evolution as a function of time in Fig. 3 for all cases. As a measure of the agreement between the retrieved/forecasted and true values of a variable, we have used the relative root mean squared error. We defined the relative root mean squared (RRMS) as

$$\mathrm{RRMS} = \frac{\sqrt{\sum_{i,j}(\hat{x}_{i,j} - x_{i,j})^2}}{\sqrt{\sum_{i,j} x_{i,j}^2}}, \tag{19}$$

where $x_{i,j}$ are the true values, and $\hat{x}_{i,j}$ are their retrieved/forecasted equivalents. The summation is carried out over the entire computational domain. Negative or zero lead times indicate the assimilation interval.

The results in Fig. 3 may be summarized as follows. Case C1 shows fairly good forecasting performance. Fig. 4 represents a measure of the rain water content, the denominator of the right-hand side of (19), as a function of time. It may be observed that for the maximum rain content, which occurs at about 10 min lead time, the rain content RRMS is about 12% (the results in the

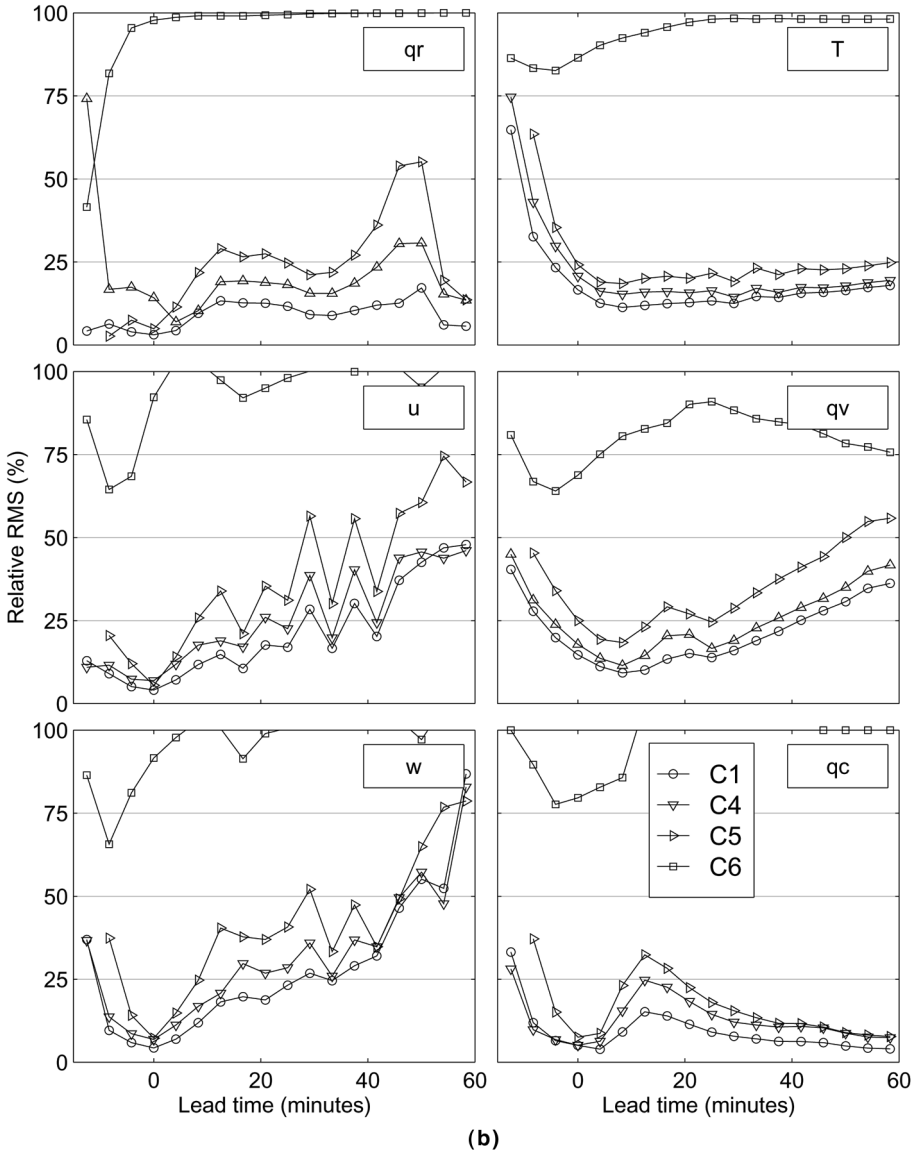


Fig. 3 (*continued*)

assimilation interval are similar to those in [17]). The RRMS seems to increase for lead times around 50 min, but this is just a consequence of a dramatic decrease of the total rain content for lead times greater than 40 min. However, it should be mentioned that a solution that corresponds to RRMS = 0 exists, but the VA framework is not able to find it. This could be caused by the optimization procedure's inability to locate the minimum of such a complex function with a large number of variables, or by a calculation of the objective function gradient which is not accurate enough. This is because the formulation presented in Section 3 is based on linearizations that become inaccurate for long assimilation intervals. Case C2 shows that, although the errors in velocity observations affect the results in the assimilation interval (negative lead times), the overall forecasting performance is similar to that of C1. A significant difference between C2 and C1 in terms of RRMS occurs at about 50 min, but as already stated, at that lead-time the total rain water content is quite low and the absolute differences are not very large. Errors in the reflectivity observation, as considered in case C3, increase the water RRMS by as much as 50% relative to C1. Unlike case C2, this increase in RRMS manifests not only for small total rain content, but also at 10–20 min lead time where the rain water content attains its maximum. Consequently, it may be stated that radar reflectivity errors have a very important impact on forecasting performance. C4 reveals that the results depend on the initial starting point in optimization. This in an indication that the objective function is complex, with many local minima, which poses problems for the gradient-based optimization procedures. Another proof in this respect, is the fact that if optimization were able to find a global

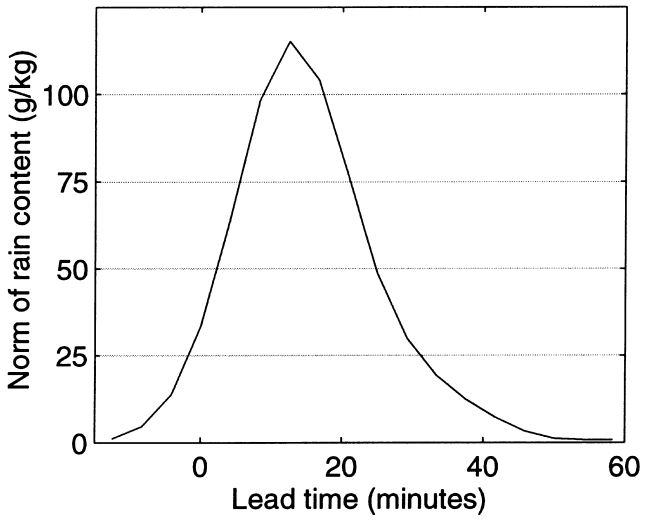


Fig. 4. Norm of rain water mixing ratio as a function of time.

minimum, the RRMS would be zero in the assimilation interval in case C1. The assimilation problem becomes better posed with an increase of the assimilation interval. This is indicated by case C5, which has a poorer performance than C1. However, the assimilation interval cannot be increased without limits as a means of improving the performance, because the volume of calculations and memory used increase accordingly, while the linear approximations on which the framework is based become poorer. This indicates the necessity of considering a background term accounting for past observations in the objective function. Finally, case C6 demonstrates that the problem is not trivial and the optimization technique, and, consequently, the development of the adjoint model, are both necessary. The error for C6 is 100% for some variables and lead times because the convection is not sustained, and the variables tend to their environmental values beyond a certain time.

Fig. 5 contains the results pertaining to cases E1 and E2. It may be noticed that the additional radar observations are beneficial for retrieval and forecasting. We remind the reader that the assimilation interval as in C1 was considered, i.e. 12.50 min, but the frequency was 25 times higher (radar observations were provided at each computational time step). As a result, the errors in retrieval and forecasting dropped about two times for all variables. When temperature observations are included in the objective function, i.e. case E2, an additional error reduction is noticed. Case E2 may be considered also a consistency test. That is because the optimization problem did not become trivial by considering additional information. This would be the case if information concerning all fields were considered, which are not in E2 where fields such as pressure, water cloud, vapor and velocity are not or just partially observed. Case E2 indicates a small error in retrieval (below 3%) for all fields. This suggests that the optimization procedure is effective when the objective function is well behaved (not exhibiting multiple minimum points similar in terms of function's value). It is worth noting that, although the errors in E2 are almost zero at the end of the assimilation interval, they grow in time and become similar to those in E1. This is an indication of the instability of the model's equations. That is, small differences in the initial conditions lead to large differences in the equations' solutions at later times. Based on these results, we may conclude that largest part of the errors originates in the ill-posedness of the problem of minimizing the function (16) with restrictions (12). In other words, no unique solution, stable to small perturbations (errors) is obtainable from radar observations only. However, as the results in experiments C1–C6 indicated, the forecasting errors induced by the ill-posedness are quite acceptable.

## 5. Summary and conclusions

In this paper, we formulated a VA procedure for incorporating radar data in cloud models and tested its utility in short term rainfall forecasting. We simulated a 2-D storm using a cloud model and synthesized radar observations to investigate the assimilation procedure performance. We considered, based on the difference between the observations and retrieved variables, various formulations for defining the objective function. The purpose of this was to identify the sources of error in retrieving (estimating) the cloud initial conditions.

We found that even in conditions of error-free observations, and four sets of observations, 4.17 min apart, the retrieval is subject to errors. Although these errors grow during forecasting, they remain within reasonable limits. It is likely that the optimization procedure is not the only component responsible for the errors in the retrieval. That is, the optimization procedure is not effective because the objective function does not have a well-defined global minimum. This is suggested by results from a retrieval based on three sets of observations. The results are better in the case with four sets of observations, because more information is available and the objective function is better defined. One possible way to make the optimization problem stable to small perturbations, is to consider a background term that includes and characterizes the uncertainty of past observation. This aspect was not studied in this paper because the simulated rain event is relatively short and the consideration of a series of assimilation intervals does not allow for the investigation of significantly long lead times. However, including the background term in the objective function is not a straightforward task, because it requires the estimation of a covariance matrix, which corresponds to the second derivative of the objective function, of a very large dimension. Future

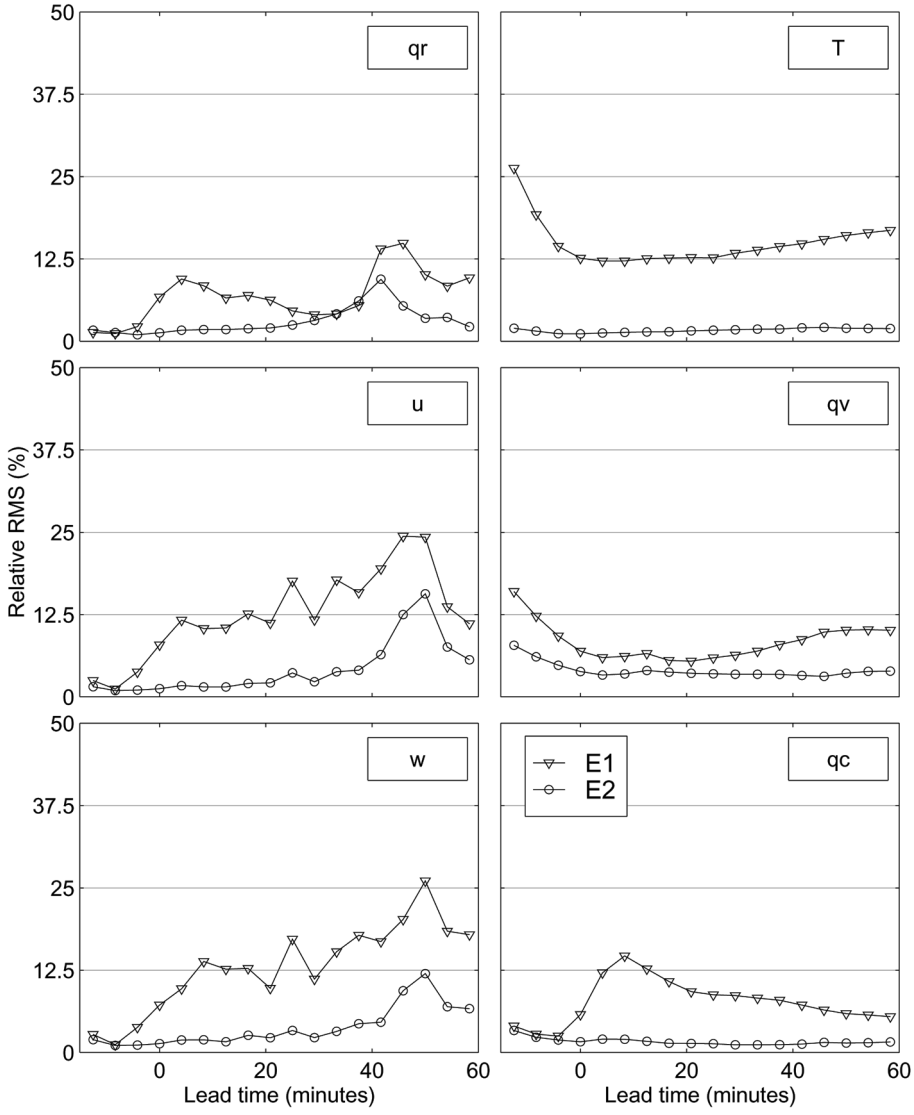


Fig. 5. Same as Fig. 3, but for cases E1 and E2.

research needs to find a tradeoff between accuracy and computational tractability.

The errors in observations affect the forecast performance. Results show that 20% errors in Doppler radial velocity do not significantly affect the results, but random errors, normally distributed with mean 0 dBZ and standard deviation 3 dBZ, in reflectivity increase the forecasting errors by about 50%. It should be mentioned that in this paper we did not consider the model errors. Results concerning the effect of model uncertainty on forecasting may be found in [9].

Nevertheless, the practical application of a VA of radar data will undoubtedly reveal new problems, because the operational cloud models, although substantially more complex than the one used in this paper, which will make the optimization problem more difficult, are still subject to errors in modeling the rain dynamics. However, the results in this paper are promising, and justify the development and application of VA techniques for rainfall forecasting.

## References

[1] Atkinson K. An introduction to numerical analysis. 2nd ed. New York: Wiley; 1989.
[2] Bao JW, Warner TT. Treatment of on/off switches in the adjoint method: FDDA experiments with a simple model. Tellus 1993;45A:525–38.
[3] Chao WC, Chang LP. Development of a four-dimensional variational analysis system using the adjoint method at GLA. 1. Dynamics. Mon Weather Rev 1992;20:1661–73.
[4] Chorin AJ. Computational fluid mechanics: selected papers. New York: Academic Press; 1989.
[5] Ciach GJ, Krajewski WF. On the estimation of radar rainfall error variance. Adv Water Resour 1999;22:585–95.
[6] Ferziger JH, Peric M. Computational methods for fluid dynamics. Berlin: Springer; 1997.

[7] Gelb A. Applied optimal estimation. Cambrigde: MIT Press; 1974.
[8] Gering R, Kaminski T. Recipes for adjoint code construction. ACM Trans Math Software 1998;24:437–74.
[9] Grecu M, Krajewski WF. Simulation study of the effects of model uncertainty in variational assimilation of radar data on rainfall forecasting. J Hydrol 2000, accepted.
[10] Houze Jr RA. Cloud dynamics. New York: Academic Press; 1993.
[11] Kessler E. On the distribution and continuity of water substance in atmospheric circulations. Meteorol Monogr 10. Boston: American Meteorological Society; 1969.
[12] Klazura GE, Imy DA. A description of the initial set of analysis products available from the NEXRAD WSR-88D system. Bull Am Meteorol Soc 1993;74:1293–311.
[13] Lee RL, Leone Jr JM. A modified finite element model for mesoscale flows over complex terrain. Comput Math Apllic 1988;16:41–56.
[14] Liu DC, Nocedal J. On the limited memory BFGS method for large-scale optimization. Math Programming 1989;45:503–28.
[15] Ogura Y, Takahashi T. Numerical simulation of the life cycle of a thunderstorm cell. Mon Weather Rev 1971;99:895–910.
[16] Sun JZ, Crook A. Wind and thermodynamic retrieval from single-doppler measurements of a gust front observed during PHOENIX-II. Mon Weather Rev 1994;122:1075–91.
[17] Sun JZ, Crook NA. Dynamical and microphysical retrieval from Doppler radar observations using a cloud model and its adjoint. 1. Model development and simulated data experiments. J Atmos Sci 1997;54:1642–61.
[18] Thomas JW. Numerical partial differential equations. New York: Springer; 1995.
[19] Tremolet Y, Le FX. Parallel algorithms for variational data assimilation and coupling models. Parallel Comput 1997;22:657–74.
[20] Verlinde J, Cotton WR. Fitting microphysical of non-steady convective clouds to a numerical model: an application of the adjoint technique of data assimilation to a kinematic model. Mon Weather Rev 1993;21:2776–93.
[21] Wallace JM, Hobbs PV. Atmospheric science: an introductory survey. New York: Academic Press; 1977.
[22] Wilhelsom RB, Ogura Y. The pressure perturbation and the numerical modeling of a cloud. J Atmos Sci 1972;29:1295–307.